

# Controlled switching circuits based on non-linear resistive elements

R.Ch. Karimov <sup>1\*</sup>, M.K. Bobojanov <sup>1</sup>, A.N. Rasulov <sup>1</sup>, E.G. Usmanov <sup>1</sup>

<sup>1</sup>Tashkent State Technical University named after Islam Karimov, 100095, Uzbekistan, Tashkent, University St. 2A

**Abstract.** Based on the results of the analysis of resistive circuits, a new circuit of an optoelectronic contactless voltage relay is developed in the article and its application in the power supply system is considered. The possibility of controlling the operating modes of various installations for amplifying electrical signals using optothyristors is presented and methods for their inclusion in electrical circuits are given. Optoelectronic contactless voltage relays were tested under laboratory conditions to obtain input-output characteristics and capacitance voltage waveforms. Based on the improvement of the proposed circuit, a circuit of an optoelectronic contactless voltage relay is developed and provides a high degree of reliability. The proposed voltage relay circuit is simulated using the Electronics Workbench and MATLAB R2014a programs, the results of which show that the changes in the shape of the output voltage curve are close to a sinusoid and coincide with the results obtained analytically.

Currently, power non-contact semiconductor equipment is widely used, which has significantly expanded the scope of semiconductor technology in a number of areas of electrical engineering and has provided qualitatively new results, which made it possible to master a new class of electrical devices.

Based on the foregoing, there is a need for the development of a non-contact voltage relay with a simple and reliable circuit that allows switching large currents of loads. For this purpose, in this paper we consider simple nonlinear resistive circuits [1-2].

High-quality devices developed on the basis of nonlinear dynamic circuits are widely used in various fields of automation, radio electronics, computer technology and power supply systems. The non-linear electric circuit under study consists of a diode connected in series to the  $VD$  network, active resistance  $R_1$  and capacitance  $C$  and connected in parallel to this resistance circuit  $R_2$  (Fig.1) [3-5].

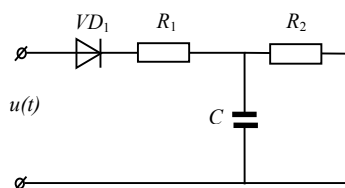


**Fig.1.** Scheme of a nonlinear electric circuit

To study the proposed nonlinear electric circuit, we use the classical method.

\* Corresponding author: [raxmatillo82@mail.ru](mailto:raxmatillo82@mail.ru)

The voltage of the circuit will change according to a sinusoidal law:

$$u = U_m \sin \omega t \quad (1)$$

We accept that the angle of inclusion of the circuit in the network is zero. Consider the transients for each diode opening. In this case, the voltage across the capacitance is described by the following equation [3, 5]:

$$u_c = U_m \cdot \frac{R_2}{R_1 + R_2} \left( 1 - e^{-\frac{R_1 + R_2}{R_1 R_2 C} t} \right) \quad (2)$$

here,  $U_m$  is the maximum value of the mains voltage;  $R_1$ ,  $R_2$  and  $C$  circuit elements.

We take the characteristic of the diode ideal and assume that  $U_{input} = U_m \sin \omega t$ . Then, from the moment  $t=0$  to  $t_1$ , the diode is open and when the condition  $0 \leq t \leq t_1$  is fulfilled, the circuit equation has the following form [3, 5]:

$$U_m \sin \omega t = R_1 i + u_c \quad (3)$$

given that, we have  $i = C \frac{du_c}{dt}$ ,

$$U_m \sin \omega t = R_1 \left( C \frac{du_c}{dt} + \frac{u_c}{R_2} \right) + u_c \quad (4)$$

From equation (4) we define  $\frac{du_c}{dt}$  and from here we get:

$$\frac{du_c}{dt} = \frac{1}{R_1 C} \left( U_m \sin \omega t - u_c \left( 1 + \frac{R_1}{R_2} \right) \right) \quad (5)$$

The differential equation of a nonlinear electric circuit described by expression (5) (Fig.1) is solved by the Lagrange method [5-8].

For an approximate solution of the differential equation of the chain, expression (5) is multiplied by  $\frac{1}{R_1 C}$  [5, 7, 9]:

$$\frac{du_c}{dt} = \frac{U_m \sin \omega t}{R_1 C} - u_c \left( \frac{1 + \frac{R_1}{R_2}}{R_1 C} \right) \quad (6)$$

By changing the equation we get:

$$\frac{du_c}{dt} + u_c \left( \frac{1 + \frac{R_1}{R_2}}{R_1 C} \right) = \frac{U_m}{R_1 C} \sin \omega t \quad (7)$$

Equating the left side of differential equation (7) to zero, we obtain [7]:

$$\frac{du_c}{dt} + u_c \left( \frac{1 + \frac{R_1}{R_2}}{R_1 C} \right) = 0$$

From here:

$$\frac{du_c}{dt} = -u_c \left( \frac{1 + \frac{R_1}{R_2}}{R_1 C} \right) \quad (8)$$

We multiply equation (8) by  $\frac{dt}{u_c}$ , integrate:

$$\int \frac{du_c}{u_c} = - \int \frac{R_1 + R_2}{R_1 R_2 C} dt \quad (9)$$

The natural logarithm of this equation is calculated as follows:

$$\ln u_c = - \left( \frac{R_1 + R_2}{R_1 R_2 C} \right) t \quad (10)$$

From here:

$$u_c = A(t) \cdot e^{-\left( \frac{R_1 + R_2}{R_1 R_2 C} \right) t} \quad (11)$$

Substituting this expression into formula (8) we obtain [7].

$$\frac{du_c}{dt} = A(t) \cdot e^{-\left( \frac{R_1 + R_2}{R_1 R_2 C} \right) t} - A(t) \cdot \left( \frac{R_1 + R_2}{R_1 R_2 C} \right) \cdot e^{-\left( \frac{R_1 + R_2}{R_1 R_2 C} \right) t} \quad (12)$$

Inserting the introduced changes in equation (7), we solve:

$$A'(t) \cdot e^{-\left( \frac{R_1 + R_2}{R_1 R_2 C} \right) t} - A(t) \cdot \left( \frac{R_1 + R_2}{R_1 R_2 C} \right) \cdot e^{-\left( \frac{R_1 + R_2}{R_1 R_2 C} \right) t} + A(t) \cdot \left( \frac{R_1 + R_2}{R_1 R_2 C} \right) \cdot e^{-\left( \frac{R_1 + R_2}{R_1 R_2 C} \right) t} = \frac{U_m}{R_1 C} \sin \omega t \quad (13)$$

After reductions, we get the following [7]:

$$A'(t) = \frac{U_m}{R_1 C} \sin \omega t \cdot \left( \frac{R_1 + R_2}{R_1 R_2 C} \right) dt \quad (14)$$

we denote  $\frac{R_1 + R_2}{R_1 R_2 C} = a$ .

We integrate equation (14) [7]:

$$A(t) = \frac{U_m}{R_1 C} \int \sin \omega t \cdot e^{at} dt \quad (15)$$

We integrate the results of equation (15) by parts:

$$I = \int \sin \omega t \cdot e^{at} dt = \int \omega \cos \omega t \cdot e^{at} dt = \frac{dv}{v} = \frac{1}{a} \cdot e^{at} \sin \omega t - \int \frac{\omega}{a} \cdot e^{at} \cos \omega t dt = \left[ \frac{\cos \omega t \cdot U}{\omega \sin \omega t} \cdot \frac{dv}{v} = \frac{1}{a} \cdot e^{at} \sin \omega t - \frac{\omega}{a^2} \cdot e^{at} \cos \omega t - \frac{\omega^2}{a^2} \int e^{at} \cdot \sin \omega t dt \right] \quad (16)$$

here,  $I = \int \sin \omega t \cdot e^{at} dt$ , the following notation is accepted:  $\sin \omega t = U$ ;  $e^{at} dt = dv$ ;  $\int u dv = uv - \int v du$ , we use the separate integration formula [7].

Simplify equation (16):

$$\int \sin \omega t \cdot e^{at} dt = \frac{1}{a} e^{at} \sin \omega t - \frac{\omega}{a^2} e^{at} \cos \omega t - \frac{\omega^2}{a^2} \int e^{at} \sin \omega t dt$$

$$\int \sin \omega t \cdot e^{at} dt \left( 1 + \frac{\omega^2}{a^2} \right) = e^{at} \left( \frac{1}{a} \sin \omega t - \frac{\omega}{a^2} \cos \omega t \right)$$

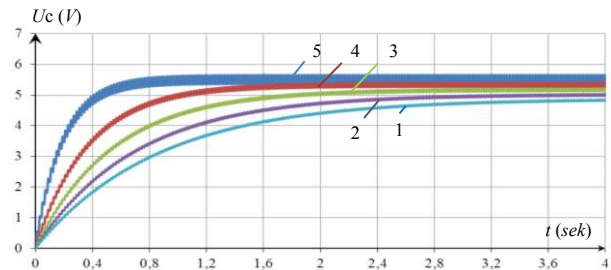
$$\int \sin \omega t \cdot e^{at} dt = \frac{a^2}{a^2 + \omega^2} \cdot e^{at} \left( \frac{1}{a} \sin \omega t - \frac{\omega}{a^2} \cos \omega t \right)$$

$$\int \sin \omega t \cdot e^{at} dt = \frac{1}{a^2 + \omega^2} \cdot (a \cdot \sin \omega t - \omega \cdot \cos \omega t) e^{at} + const \quad (17)$$

We introduce a constant in equation (17), taking into account (11) and (16) after some transformations we get [5, 7]:

$$u_c = \frac{U_m}{R_1 C} \cdot \left( \frac{1}{\left( \frac{R_1 + R_2}{R_1 R_2 C} \right)^2 + \omega^2} \right) \left( \frac{R_1 + R_2}{R_1 R_2 C} \sin \omega t - \omega \cos \omega t \right) + const \cdot e^{-\left( \frac{R_1 + R_2}{R_1 R_2 C} \right) t} \quad (18)$$

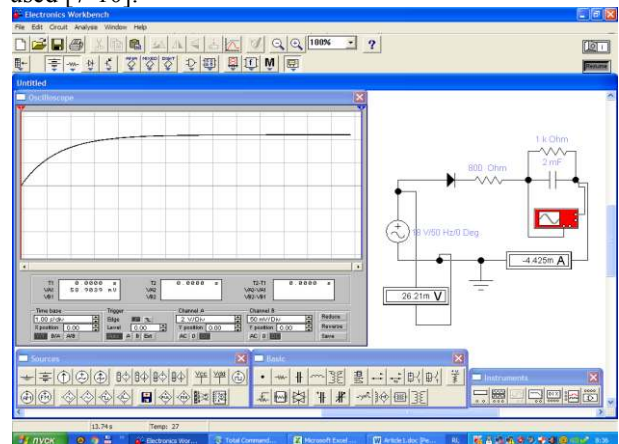
Figure 2 shows the graphs of the voltage change across the capacitance determined using formula (7).



**Fig.2.** The voltage variation curves at the capacitance  $U_c=f(t)$  with constant  $C$  and  $R_2$  and with changing parameters  $R_1$

Figure 2 shows the curves of the voltage change at the capacitance at: network voltage  $U_m=18$  V, capacitance  $C=1$   $\mu$ F, resistance  $R_2=3,0$  kOhm, the integration step  $h=0,001$ , and when the resistance  $R_1$  changes (1 – 0,3 kOhm; 2 – 0,5 kOhm; 3 – 0,8 kOhm; 4 – 1,0 kOhm; 5 – 1,2 kOhm).

To verify the reliability of the simulation results of the considered circuit, computer simulation software was used [7-10].



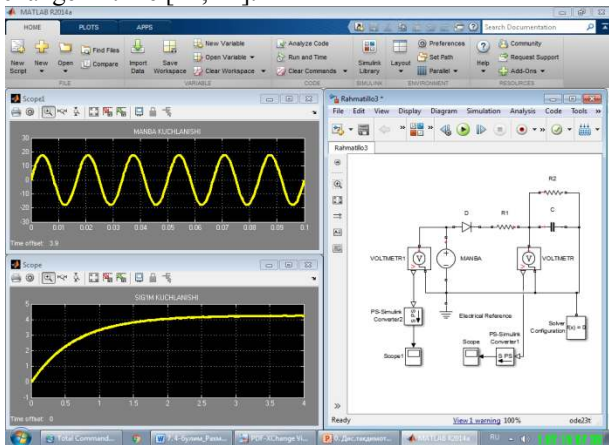
**Fig.3.** Simulation process using the Electronics Workbench software

Figure 3 shows a simulated graph of the voltage variation across the capacitance  $U_c=f(t)$ , considered in Fig.1 non-linear circuit using Electronics Workbench [6-7, 9-10, 12].

The graph of changes in the capacitance voltage  $U_c=f(t)$  is shown in Fig.4 [13].

In the analysis time, by the Simulink block of the MATLAB R2014a program, a nonlinear electrical circuit (Fig.1), the process progresses over time, the results show that this program makes it possible to conduct

more data for the analysis of the processes of voltage change in time [11, 14].



**Fig.4.** The modeling process using the program MATLAB R2014a

Figure 5 shows a comparison of the results obtained by mathematical modeling methods and programs: *a* - Electronics Workbench; *b* - MATLAB R2014a and *c* – analytical research method.

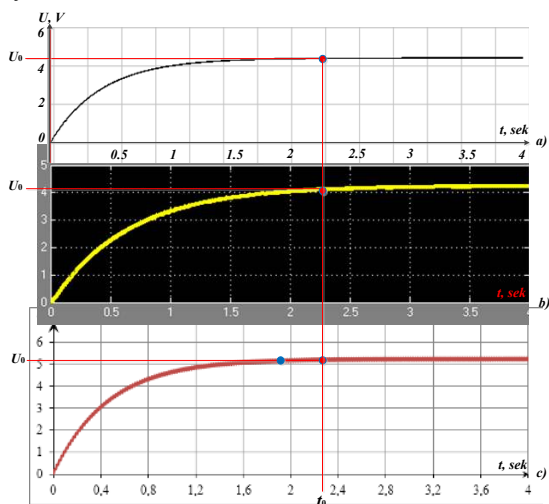


**Fig.5.** Comparison of the results of analysis of a nonlinear electric circuit

An analysis of the results of the graph of the voltage across the capacitance shows that the difference between the Lagrange methods and modeling using the Electronics Workbench and MATLAB programs is 1.5-2%. This is explained by the input of a constant value when solving the circuit under consideration by the Lagrange method. The results obtained by modeling a nonlinear electric circuit and the obtained analytical methods give the same results and coincide with the theoretical curves [6].

The shape of the load current can be influenced by controlling the opening angle of the thyristor. When the phase shift between the load current and the control signal is equal to zero, the curve of the load current will be in the form of a sinusoid. Thus, in order to ensure a sinusoidal shape of the current and voltage curves on the load, it is necessary to apply a signal to open the thyristor when the current passes through zero [4, 15].

Compared to electromagnetic installations, optoelectronic relays differ in reliability, durability and resistance to transient and frequency characteristics, improved technical and economic indicators and speed, makes it possible to use transformer windings and relay protection installations without switching special devices [3, 16-17].

The implementation of the optoelectronic contactless voltage relay using a thyristor and an optocoupler improves weight and dimensions. Figure 6 shows a circuit diagram of an optoelectronic contactless voltage relay with a sinusoidal waveform of a voltage across a load [4].

Consider the operation of an optoelectronic contactless voltage relay. The non-contact voltage relay consists of a diode bridge  $VD_2-VD_5$  connected to a power source in series with the load  $R_{load}$ , into the diagonal of which the thyristor  $VT_2$  is connected. The relay is also equipped with a capacitor  $C$ , a thyristor  $VT_1$ , three resistors  $R_1, R_2, R_3$ , a thyristor optocoupler  $VU$  and a diode  $VD_1$ . The control electrode of the first thyristor  $VT_2$  is connected through a resistor  $R_3$  to the capacitor plate  $C$  and the cathode of the thyristor optocoupler  $VU$ . The second lining of the capacitor  $C$  is connected to the cathodes of the thyristor  $VT_2$ , the cathode of the second thyristor  $VT_1$  and the second terminal of the supply network. The anode of the thyristor  $VT_1$  is connected to the cathode of the diode of the optocoupler  $VU$ , the anode of which is connected to the output of the resistor  $R_2$ . The second output of the resistor  $R_2$  is connected to the anode of the thyristor of the optocoupler  $VU$  and the first output of the resistor  $R_1$  also has connections to the first terminal of the supply network. The second output of the resistor  $R_1$  is connected to the anode of the diode  $VD_1$ , the cathode of which is connected to the control electrode of the thyristor  $VT_1$  [15-16].

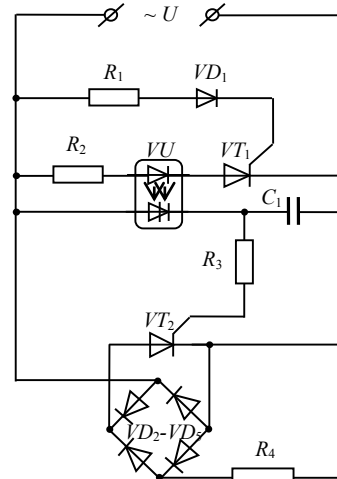


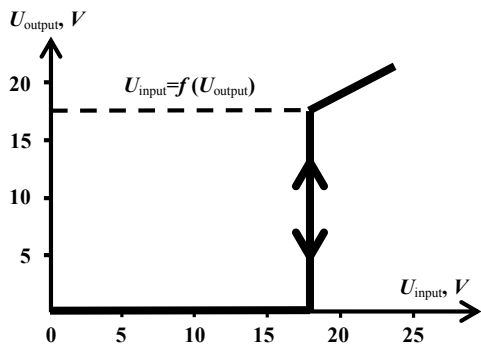
**Fig.6.** Schematic diagram of the optoelectronic contactless voltage relay

Consider the operation of an optoelectronic contactless voltage relay. When the unlocking signal at the control electrode reaches a value sufficient to unlock the thyristor, the thyristor  $VT_1$  opens with an opening angle of  $90^0$  and connects the diode of the  $VU$  optocoupler to the network through a resistor. This leads

to the opening of the thyristor of the optocoupler  $VU$  and the flow of current through the diode of the optocoupler, thereby leading to the opening of the thyristor of the optocoupler  $VU$ , and turns on the capacitor  $C$ . Since a constant signal is supplied from the capacitor  $C$  through the resistor  $R_3$  to the control electrode of the thyristor  $VT_2$ , it remains open, and a sinusoidal current flows through the load  $R_4$ . The triggering of thyristors  $VT_1$  is controlled by changing the parameter of the resistor  $R_1$  [16-17].

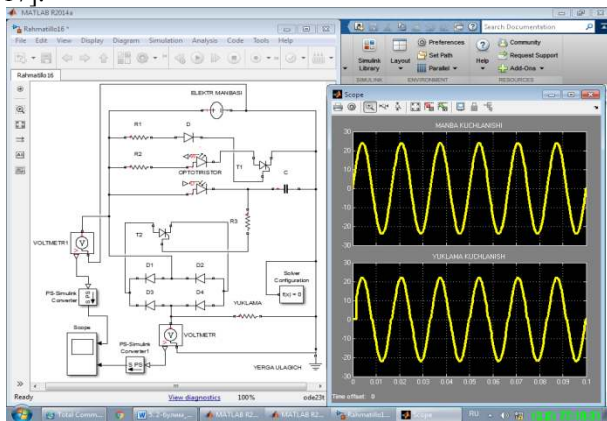
This optoelectronic contactless voltage relay has been tested in the laboratory of the Department of Power Supply of the Energy Department of the Tashkent State Technical University named after Islam Karimov. In this case, thyristors  $KU202I$ ,  $KU201I$ , respectively, were used as thyristors  $VT_1$ ,  $VT_2$ ,  $D226B$ , as diodes  $VD_1$ , as resistors  $R_1$ ,  $R_2$ ,  $R_3$ ,  $R_4$ , respectively, resistors of 820 Ohms, 15 kOhm, 3.8 kOhm, 16 kOhm, capacitor  $C$  with a capacitance of 1  $\mu F$  as capacitance  $C$ ,  $AOU103V$  thyristor optocoupler,  $VD_2-VD_5$  diode bridge -  $KTs402E$  used as optocouplers. Experimental studies have shown that the load  $R_4$  was included in the network at a voltage of 18 V. The shape of the load voltage curve is sinusoidal [16-17].

Figure 7 shows the input-output voltage characteristic of an optothyristor non-contact voltage relay and it.



**Fig.7.** The characteristic "input-output" voltage optoelectronic proximity voltage relay

Using the MATLAB R2014a program, the circuit of the optoelectronic contactless voltage relay is shown (Fig.6), the results of which are shown in Fig.8 [11, 16-17].



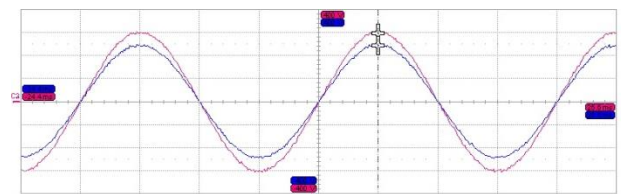
**Fig.8.** Modeling of an optoelectronic contactless voltage relay

Thus, the optoelectronic contactless voltage relay has a sinusoidal shape at the output [16-18].

In the laboratory of the Department of Power Supply, experimental studies were conducted using a digital oscilloscope of the LeCroy WaveRunner 64 Xi-A type (USA) and the voltage amplitude value was taken.

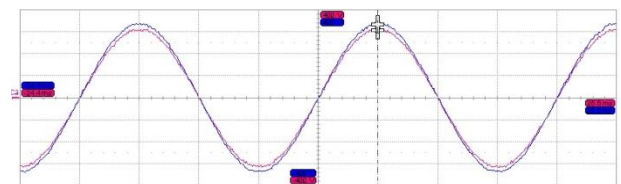
Experimental waveforms are shown, the input voltage variation curves within the range of 176÷241 V, while the output voltage varies within the range of 217÷224 V. The results of the experiments show that the proposed voltage stabilizer, depending on the change in the voltage of the network, provides voltage stability at the load, i.e. within  $\pm 2\%$  of the nominal [19-20].

Figure 9-10 shows the oscillograms of the input-output voltage, the stabilizer for active load.



**Fig.9.** The waveform of the voltage input-output voltage stabilizer for active load:  $U_{input}=175$  V;  $U_{output}=214$  V

Figure 9 shows the oscillogram of the voltage change at  $U_{input}=175$  V (deviation from the nominal -20,4%) and load voltage  $U_{output}=214$  V (deviation from the nominal -2,72%), the input-output voltage difference is 39 V.



**Fig.10.** The waveform of the voltage input-output voltage regulator for an active load:  $U_{input}=241$  V;  $U_{output}=224$  V

Figure 10 shows the oscillogram of the voltage change at  $U_{input}=241$  V (deviation from the nominal value of 8,71%) and the voltage at the load  $U_{output}=224$  V (deviation from the nominal value of 1,78%), the input-output voltage difference is 17 V.

The results of the analysis of the voltage waveform show that, when the input voltage varies from -20,4% to +8,71%, the output of the voltage regulator changes from -2,72% to +1,78%. Thus, the developed prototype voltage stabilizer meets the requirements of the state standard [19-20].

Thus, the goal and objectives set in this scientific work are obtained, such an optoelectronic contactless voltage relay has been developed; for use in the switching control system of the magnetizing windings of a boost transformer [16].

The tested prototype of the voltage stabilizer provides a deviation of the voltage at the load within the permissible range of  $\pm 5\%$  from the nominal one, which leads to an improvement in the quality of electricity.

## Conclusion

To analyze the dynamic processes of a nonlinear electric circuit, a solution to the differential equation is developed.

For the analysis of a nonlinear electric circuit, it is recommended to use a numerical method for solving the differential equation of state of a circuit. Using computer technology, this circuit was studied vertically experimentally and it was found that the time to establish the voltage on the capacitance depends on the value of the parameters of the diode-capacitive circuit.

Based on the improvement of the proposed circuit, a circuit of an optoelectronic contactless voltage relay is developed that eliminates false alarms and provides a high degree of reliability.

The simulation of the proposed voltage relay circuits is performed using the MATLAB R2014a program, the results of which show that changes in the shape of the output voltage curve are close to a sinusoid and coincide with the results obtained analytically.

Experimentally, using the LeCroy WaveRunner 64 Xi-A type oscilloscope, the proposed voltage stabilizer was tested and it was determined that the use of this stabilizer reduces the starting torque of the active-inductive load by 0,2 sec.

## References

1. ES Filippov, Textbook, Energy, 504 (1985).
2. MK Bobojanov, RCh Karimov, Bulletin of TSTU, **4(101)**, 53-57 (2017).
3. MK Bobojanov, EG Usmanov, EH Abduraimov, RCh Karimov, JESR, **1-2**, 210-212 (2018).
4. AN Rasulov, RCh Karimov, JEE, **4**, 174-178 (2015).
5. RCh Karimov, Collection of materials of the IV international scientific conference "Modern Trends in Technical Sciences", 33-35 (2015).
6. EG Usmanov, AN Rasulov, RCh Karimov, DGU 05406 (2018).
7. RCh Karimov, EG Usmanov, AN Rasulov, MR Ruzinazarov, DGU 06134 (2019).
8. WJ Cunningham, Textbook, Gosenergoizdat, 456 (1962).
9. VP Sigorsky, AI Petrenko, Textbook, Publishing. 2nd, Soviet Radio, 608 (1976).
10. II Aliev, Textbook House of Radio, 112 (2003).
11. VV Teryokhin, Textbook, Kuzbassvuzizdat, 376 (2004).
12. <http://studentlib.com>, <http://radio.bobrodobro.ru/10215>
13. VS Scherbakov, AA Ruppel, VA Glushets, Textbook, Publishing House, 160 (2003).
14. AM Namestnikov, Methodological guidelines, UISTU, 72 (2004).
15. MM Fayziev, NA Kurbonov, IN Karimov, JYS, **6**, 215-219 (2016).
16. EG Usmanov, EKh Abduraimov, RCh Karimov, Patent of Uzbekistan. IAP 05122 (2015).
17. EKh Abduraimov, RCh Karimov, INNOVATION-2016, 128-129 (2016).
18. AX Sulliev, RCh Karimov, JTREI, **4**, 149-154 (2018).
19. Interstate standard GOST 32144-2013.
20. The state standard of Uz. is O'zDSt 1044:2003.